Quantum Manipulation Using Light-Atom Interaction

Academic and Research Staff
Professor Vladan Vuletic

Visiting Scientists and Research Affiliates
Dr. Chiara D'Errico, Dr. Branislav Jelenkovic, Dr. Sebastian Hofferberth, Dr. Fedja Orucevic, Dr. Matthias Scholz

Graduate Students
Marko Cetina, Wenlan Chen, Andrew Grier, Ian Leroux, Thibault Peyronel, Jonathan Simon, Monika Schleier-Smith, Haruka Tanji

Undergraduate Students
Alexander Papageorge, Tracy Li, Ken Wang

Support Staff
Joanna Keseberg

1. All-optical switching with a few hundred photons

Sponsors
ARO Harvard
Project in collaboration with Prof. Mikhail Lukin's group at Harvard University

Interactions between weak optical pulses at the single-photon level represent the fundamental limit of nonlinear optical science, and reaching this regime has been a long-standing goal, investigated over the last three decades [1]. In addition to fundamental interest, these efforts are stimulated by potential applications in quantum information science [2]. Examples include photon-photon switches, and all-optical transistors at the single-photon level.

In general, such nonlinear interactions are very difficult to achieve, as they require a combination of large optical nonlinearity, long atom-photon interaction times, low photon loss, and tight confinement of the light. Here, we demonstrate a novel approach that enables strong, coherent nonlinear interactions between few-photon pulses. Our approach makes use of a mesoscopic ensemble of a few hundred cold rubidium atoms trapped inside a microscopic hollow-core photonic-crystal fiber (PCF) [3]. The tight transverse confinement of the atoms and of the light within the same one dimensional waveguide enables strong atom-photon interactions. We investigate electromagnetically induced transparency (EIT) in a mesoscopic regime involving small numbers of atoms and photons [1], and demonstrate nonlinear all-optical switching with a few hundred photons per switching pulse, and one photon per target pulse.

For simultaneous confinement of atoms and light on a length scale d, the interaction probability between a single atom and a single photon of wavelength λ scales as $p \sim \lambda^2/d^2$, and can, under realistic conditions, approach few percent. In turn, this medium can be manipulated by pulses containing about a hundred photons. Such a medium enables strong atom-photon and photon-photon interaction.

Simultaneous implementation of all requirements for few-photon nonlinear optics has until now only been feasible in the context of cavity QED, where single atoms are trapped within narrow-band, high-finesse cavities [4]. Over the last decade, major progress in this area has been achieved, with several experiments demonstrating nonlinear optical phenomena with single intracavity photons [5–7]. However, these experiments remain technologically challenging and must compromise between cavity bandwidth, mirror transmission, and atom-photon interaction strength. As a result, large nonlinearities are currently accompanied in these systems by substantial losses at the input and output of the cavity. In this work, an alternative, cavity-free approach involving propagating fields in PCF is investigated. Recently, hollow-core PCF filled with molecular gas has been used for significant enhancements of efficiency in processes such as wavelength conversion [8] and four-wave mixing [9]. Several groups have also successfully loaded atomic vapor into a PCF, for applications such as atomic guiding [10]. The recent observations of electromagnetically induced transparency in room-temperature rubidium with a nanowatt-level control fields [11] has demonstrated that these systems are highly promising for low-light-level nonlinear optics.

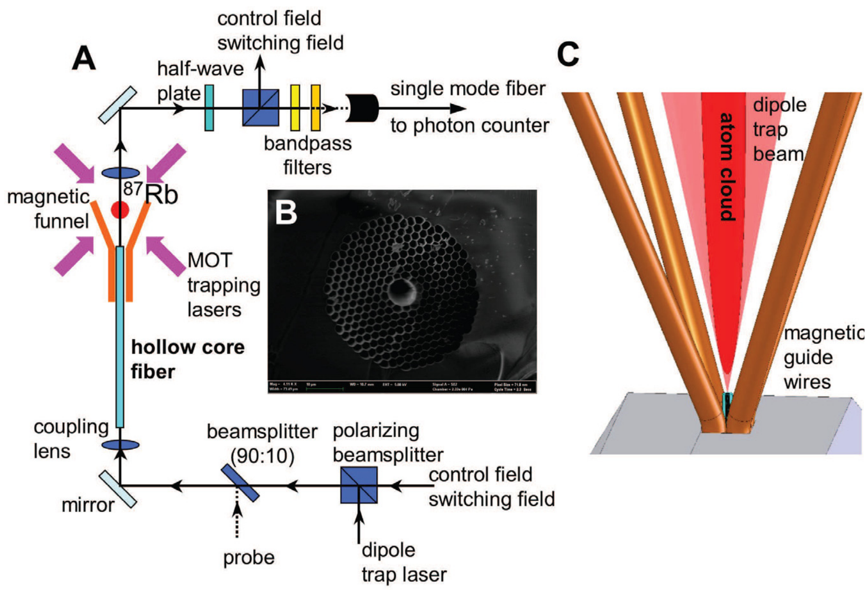

Figure 1: **Loading and probing of the atoms inside the hollow-core photonic-bandgap fiber. (A)** Schematics of the experimental setup. **(B)** Scanning-electron-microscope image of the fiber cross section. The diameter of the central hollow region is 7μm. **(C)** Inside the fiber, the atoms are transversally trapped by a single guided-beam optical trap. After exiting the top end of the fiber the divergent beam creates an additional funnel potential guiding the atoms into the fiber core from a distance up to ~ 100 μm. **(D)** Transmission of the fiber as a function of probe frequency. Red points show the absorption profile with the dipole trap on continuously. The observed inhomogeneous broadening and shifting of the absorption line is due to the spatially varying AC stark shift induced by the dipole trap. **(E)** Black points show the absorption profile for the modulated case. Here, homogeneous broadening is caused solely by the large optical depth of the system (OD = 30 for the shown data). The dipole trap is only modulated during the probing sequence and the frequency of the modulation is chosen sufficiently high, so that the atomic motion cannot follow the potential variation. Individual probe pulses of 100-500 ns duration contain ~1 photon on average.

Our experimental apparatus (Fig. 1A) makes use of a 3 cm-long piece of hollow core PCF vertically mounted inside an ultra-high vacuum chamber together with two short focal length lenses that allow coupling of light into the guided mode of the fiber. A laser-cooled cloud of ^{87}Rb atoms is collected into a magneto-optical trap (MOT), focused with a magnetic guide, and loaded into the hollow core of the PCF. Once inside, the atoms are radially confined by a dipole trap formed by a single beam guided by the fiber itself. The dipole trap is red detuned from the rubidium D_2 line (λ= 780 nm), such that the atoms are pulled towards the intensity maximum of the trapping light [12], i.e. towards the center of the hollow core. Inside the fiber, the small diameter of the guided mode allows for strong transverse confinement (trapping frequencies $\omega_t/(2\pi) \approx$ (50-100) kHz) and deep trapping potential (~10 mK) at guiding-light intensities of a few milliwatts.

To probe the atoms in the fiber, we monitor the transmission of a very low intensity (~1 pW) probe beam coupled into the PCF (Fig. 1A). This probe can be frequency tuned over the resonance absorption lines of rubidium, and its transmission is detected by a single-photon counter. The signature of atom loading into the PFC is a unique absorption profile shown in figure 1D. The dipole trap light introduces a power dependent, radially varying AC-Stark shift, which results in inhomogeneous broadening and frequency shift of the absorption profile (red data in Fig. 1D). Comparison with the absorption profile calculated from the dipole trap parameters verifies that the atoms are loaded inside the fiber. For the optical experiments described below, we avoid the unwanted perturbation of the absorption profile by synchronously modulating the dipole trap and the probe beam out of phase (Fig. 1E). The modulation at a rate faster than trapping frequency allows the atoms to interact with the probe photons only when the dipole trap is off, while the time-averaged optical trap still prevents them from colliding with the fiber wall.

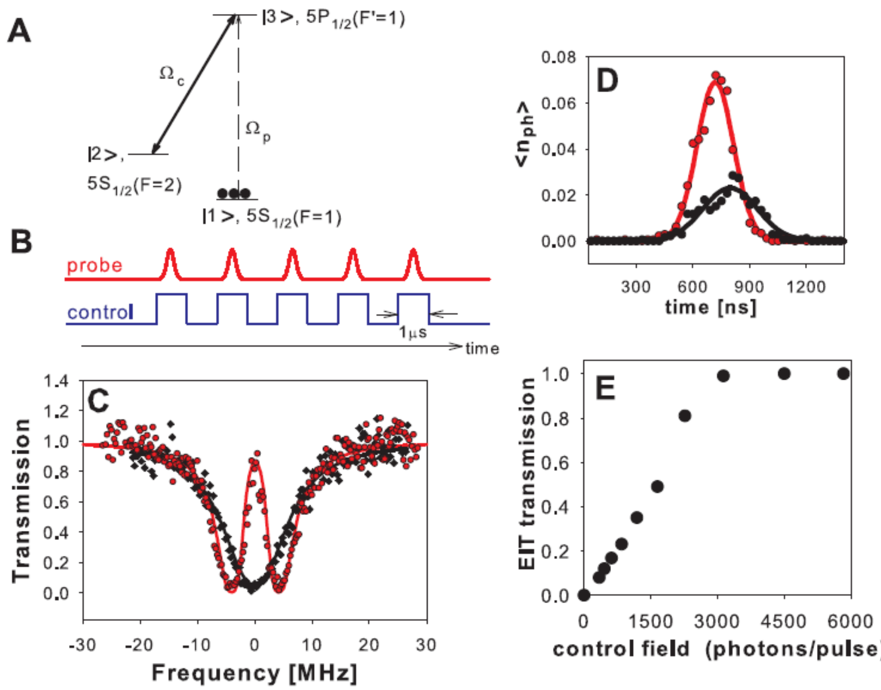

Figure 2: **Electromagnetically induced transparency in a mesoscopic atomic ensemble. (A)** Three-level lambda scheme for the realization of EIT. **(B)** Both probe and control field are broken into a set of ~100 synchronized pulses sent through the fiber during the off-times of the dipole trap which is modulated at 500 kHz. The control-field pulses have rise times of 40 ns and duration of 1 μs, while the probe pulses have Gaussian envelopes with half width t_p ~ 150 ns to reduce their bandwidth. **(C)** Probe transmission through the fiber without (black data points) and with (red data points) control field. Solid lines are fits to the data. From such fits, we obtain the dephasing rate of the EIT coherence γ_{12} = 0.050(4) MHz, as well as the control field Rabi frequencies Ω_c corresponding to different degrees of transparency. **(D)** Individual pulse delay: the reference pulse (red) is obtained without atoms, while the EIT pulse (black) is delayed by ~ 100ns for control pulses containing ~ 1000 photons. Individual probe pulses contain on average ~ 2 photons. **(E)** Transmission of the probe pulses on resonance as a function of average number of photons in the control-field pulse. Full transparency of the atomic medium is achieved with ~ 2000 control photons.

When using this technique and scanning the probe laser over a particular $F \rightarrow F'$ hyperfine transition, we observe a typical absorption profile as shown in figure 1D (black data points). Since the atomic sample is cold and dilute, the shape of this resonance is completely deterined by the natural line profile of the transition, $T=\exp[-OD/(1+4(\Delta/\Gamma_e)^2)]$, where Γ_e is the lifetime of the excited atomic state, and Δ is the detuning of the probe laser from resonance. The optical depth

$OD=N_a\sigma_{eg}/(\pi w^2)$, i.e. the on-resonance attenuation of the probe beam, is a figure of merit for coupling between the atomic ensemble and the photons. Here, N_a is the number of atoms in the fiber, σ_{eg} the atomic cross section for the probed transition, and w=1.9(2) μm is the beam waist of the guided light inside the fiber. From this we conclude that ~100 atoms inside the fiber create an optically dense medium (OD=1). Fitting the above expression to the profile shown in Fig. 1D yields OD=30, which corresponds to $N_a \approx 3000$ atoms loaded into the fiber.

We now turn to coherent interaction between few atoms and photons in our system. To this end, we demonstrate electromagnetically induced transparency (EIT) [13, 14], coherently changing the atomic properties to make the opaque sample inside the fiber transparent for a resonant probe beam. For this we consider the 3-state 'Lambda' configuration of atomic states shown in figure 2A. In the presence of a strong control field, the weak probe field, resonant to the $|1\rangle \rightarrow |3\rangle$ transition, is transmitted without loss. The essence of EIT is the creation of a coupled excitation of photons and atomic spins ("dark-state polariton") [15] that propagates through the atomic medium with greatly reduced group velocity [16], and can be optically manipulated with a high degree of control.

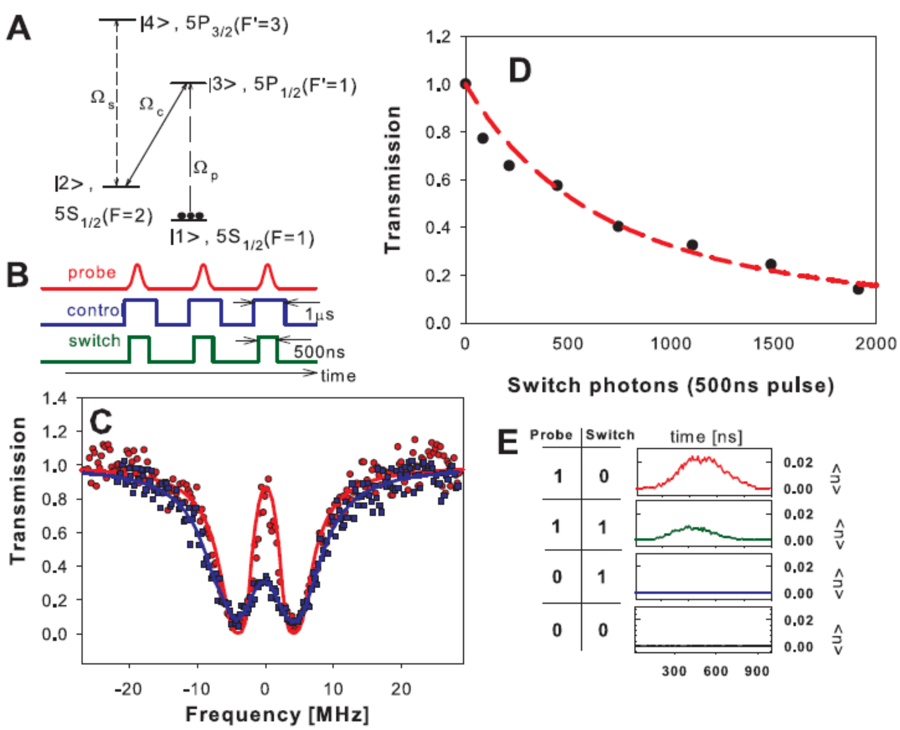

Figure 3: **All-optical coherent switch. (A)** Four-level system for photon switching. **(B)** The timing sequences for probe, control, and switching fields. **(C)** Probe transmission through the fiber without (red) and with (blue) switching field present. Solid lines are fits to a simple model. The presence of the switch pulse reduces the EIT transmission. **(D)** Measured normalized transmission versus average switch photons per pulse. The solid line is the theoretical prediction based on experimental parameters. **(E)** Truth table of the coherent switch, showing the detected photons in the output port of the switch system as a function of the presence of the probe and switch-field pulses. Data are presented for probe pulses containing on average ~ 2 photons and ~1/e attenuation of transmission.

To demonstrate EIT, we first prepare the atoms in the F=1 ground state, and then probe the medium with a linearly polarized probe tuned to the F=1 → F'=1 transition. In the absence of the control beam, the medium is completely opaque at resonance (Fig. 2C, black data). In contrast, when a co-propagating control field resonant with the F=2 → F'=1 transition is added, the atomic ensemble becomes transparent near the two-photon resonance (Fig. 2C, red data). Figure 2D shows the individual pulse shape and its transmission and delay due to reduced group velocity v_g inside the atomic medium. For a probe pulse of duration ~300 ns we observe a delay approaching 100 ns, corresponding to $v_g \approx 3$ km/s. Finally, figure 2E shows the resonant probe transmission as a function of the average number of photons contained in each control field pulse. Remarkably, control pulses containing ~2000 photons are sufficient to achieve almost perfect transparency of the otherwise opaque system. The sensitive nature of the quantum interference underlying EIT enables strong non-linear coherent interaction between the dark-state polariton and additional light fields, which can be interpreted as an effective photon-photon interaction [17–19]. An efficient nonlinear optical switch based on this idea can be realized by adding an additional switch field coupling the state $|2\rangle$ to an excited state $|4\rangle$ to the EIT 'Lambda'-system (Fig. 3A), as proposed by Harris and Yamamoto [20]. In this scheme, the switching photons interact with flipped atomic spins within the slow dark-state polariton, causing a simultaneous absorption of a probe and a switching photon.

In our experiment, an additional switching field on the D_2 F=2 → F'=3 transition (Fig. 3A) controls the transmission through the EIT medium. Switching is achieved when all three involved light fields (probe, control and switching field) are overlapping in time (Fig.3B). As shown in Figure 3C, in the absence of the switching field (red data), we observe high transmission of the probe beam on resonance due to EIT. When the switch field is turned on, this transmission is reduced. The strength of this reduction depends exponentially on the switch field intensity (Fig. 3D). In particular, we find a 50% reduction of the initial transmission for a total number of ~500 switch photons per pulse. Figure 3E presents the truth table of our switch. In the case of no probe pulse (0/0 and 0/1 settings of the switch) only background noise photons of the control field are detected, which are easily suppressed to be orders of magnitude smaller than the single photon per probe pulse.

The number of required switch photons can be further reduced by increasing the *OD* of the ensemble (e.g. by improving the atom loading efficiency). Ultimately, for sufficient *OD*, the whole probe pulse is stored simultaneously inside the medium as atomic excitation [15]. In particular, in the case of a single slow probe photon, the polariton contains only a single atomic spin at any time. Consequently, absorption of a single switch photon is required to destroy the atomic excitation. This process occurs with probability $p \sim \lambda^2/d^2$. Hence, the system is transparent for the probe beam in the absence of the switching field, and opaque when $n \sim 1/p$ switching photons are present. This would achieve the maximum switching efficiency possible for this scheme, which for the particular level scheme used here corresponds to about $n \sim 1/p \sim 100$ photons.

Our experimental demonstrations introduce a novel physical system that opens up unique new prospects in quantum and nonlinear optics. For example, our system can be used to implement efficient photon counting [22] by combining photon storage with spin-flipped atom interrogation via the cycling transition. Further improvements in nonlinear optical efficiency are possible using stationary pulse techniques [23]. In that case, a standing wave control field formed by two counter-propagating beams is used to form an EIT Bragg grating, in which the probe pulse can be completely stopped with non-vanishing photonic component. In particular, application of this scheme inside the PCF has been proposed for single-photon controlled switching, with probability of interaction between two single photons scaling as $OD\lambda^2/d^2$ [24]. With relatively modest improvement in atom loading, achieving deterministic nonlinear switching with two guided photons appears within reach. Such systems may have diverse applications in quantum communication and information processing [2]. Finally, the present demonstration opens up the possibility to create strongly interacting many-body photon states [25], which may give new insights into the physics of non-equilibrium strongly correlated systems.

2. Cavity cooling of a single trapped ion and resonator-coupled ion array

Sponsors
ARO QUEST
National Science Foundation – Award ID number PHY 0653414
Project in collaboration with Prof. Isaac Chuang

In the laser cooling of atoms or ions [26-29], methods of particular interest are those that do not destroy the quantum mechanical coherences in the internal degrees of freedom, where the quantum information is stored. For example, in trapped-ion quantum information processing [30], it is necessary to cool the center-of-mass motion of the ions without affecting the coherence between internal hyperfine or electronic levels. This has been accomplished by sympathetic cooling of the processing ion using a laser cooled ion of another species [31].

Cavity cooling is an alternative, all-optical method that may allow one to cool a particle without causing decoherence of the internal states. When a particle is illuminated with monochromatic laser light, the spectrum of the scattered light is broadened out around the incident frequency due to the particle's motion. For a weakly confined atom, the spectrum is broadened by the Doppler effect, while in the limit of strong confinement discrete sidebands appear that are spaced by multiples of the trap frequency. In either case, if an optical resonator is used to enhance selected portions of the emission spectrum, such that the average emission frequency exceeds that of the incident light, energy conservation implies that the particle is cooled in the scattering process (cavity cooling) [32-34]. Unlike conventional Doppler cooling [35], cavity cooling does not require the incident light to be matched to an atomic resonance, and can in principle be performed with non-resonant light. As light scattered far off resonance carries no information about the atom's internal state [36,37], such a process can potentially cool an atom without destroying a quantum superposition of internal states.

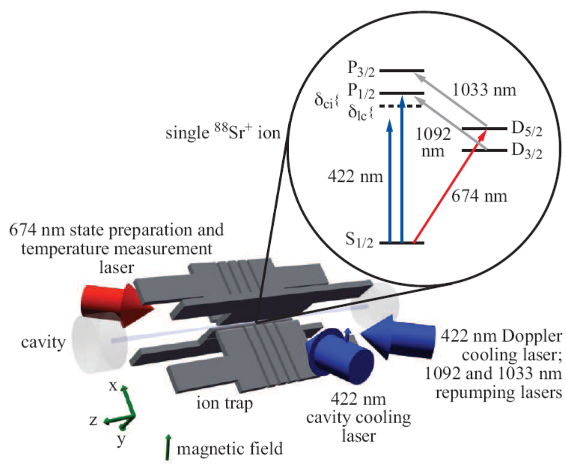

Figure 4. Schematic of the experimental setup. A single $^{88}Sr^+$ ion is confined in the center of a linear RF Paul trap and coupled to an optical resonator oriented along the trap axis. The inset shows the ion energy levels (solid lines) and the cavity resonance (dashed line).

Cavity cooling relies on the frequency discrimination provided by the resonator, and hence cooling to the quantum mechanical ground state of the external trapping potential is possible only when the trap frequency ω exceeds the cavity linewidth κ (cavity resolved-sideband regime) [34]. In the resolved-sideband regime cooling is achieved by tuning the resonator an amount ω to the blue of the incident light, such that scattering events into the cavity correspond to transitions $|n\rangle \rightarrow |n-1\rangle$ that lower the motional quantum number n. The steady-state temperature is then set by the competition between cooling by photons scattered into the cavity and recoil heating by photons scattered into free space [34]. Denoting the probability of scattering into a resonant cavity relative to free space by the cooperativity η, the steady-state average vibrational quantum number n_0 in the resolved-sideband regime $\kappa \ll \omega$ is given by [33,34] $n_0 = C/\eta$, where C is a dimensionless factor of order unity that depends on the cooling geometry. Thus in the strong-coupling regime $\eta \gg 1$ cooling to the motional ground state is possible, while for moderate coupling $\eta < 1$ the cooling is limited by the cooperativity.

Cavity cooling has been demonstrated in the weak-confinement regime $\omega \ll \kappa$ with single trapped atoms without directly measuring the atomic temperature [38-40], and with atomic ensembles in a different parameter regime of collective coupling [41,42]. Here, using a single trapped $^{88}Sr^{+}$ ion in the resolved-sideband regime, we measure cavity heating and cooling rates and the steady-state cooling limit, and observe parameter-free agreement with a rate equation model for cavity cooling [33,34].

The setup and level scheme for $^{88}Sr^{+}$ are indicated in Fig. 4. We use a linear Paul trap with trap frequencies near 1 MHz. A 5-cm-long optical cavity of finesse $F = 2.56(1) \times 10^4$, is oriented along the ion trap axis, while the cavity cooling laser (λ = 422 nm) is perpendicular to the ion trap axis. The cooperativity at an antinode of the cavity for a two-level atom is $\eta_0 = 24F/(\pi k^2 w^2) = 0.26$, where $k = 2\pi/\lambda$ is the wavenumber, and w = 58 μm the cavity mode waist [34]. The effective cooperativity for the actual transition used in $^{88}Sr^{+}$ is reduced by several effects, and is experimentally determined to be $\eta = 0.019$, placing the system in the weak-coupling regime.

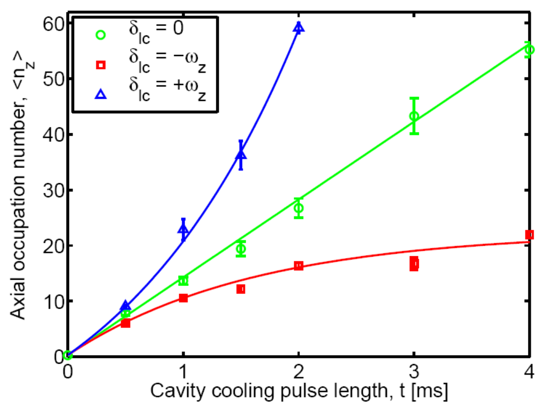

Figure 5. Cavity cooling dynamics. The ion is sideband cooled to the three-dimensional motional ground state using standard sideband cooling on a narrow optical transition. Then a cavity cooling pulse with detuning $\delta_{lc}=0$ (carrier), $\delta_{lc}=-\omega_z$ (red axial sideband), or), $\delta_{lc}=+\omega_z$ (blue axial sideband) is applied, and the mean number of motional quanta in the z mode is measured. The three lines are a simultaneous fit to the model of Ref. [34] with no free parameters.

We investigate one-dimensional cavity cooling along the z direction by measuring separately the recoil heating rate, as well as the cavity cooling and heating rates for pumping on the cavity red and blue motional sidebands, respectively. To realize a situation that allows simple quantitative comparison with the theoretical model for cavity cooling [33,34], we prepare the ion in its motional ground state by standard sideband cooling on the narrow $S_{1/2} \rightarrow D_{5/2}$ transition. We then apply the cavity cooling for a variable time. Finally, the mean vibrational quantum number $\langle n \rangle$ is determined by measuring the Rabi frequencies of the red and blue motional sidebands on the narrow $S_{1/2} \rightarrow D_{5/2}$ transition [30].

Fig. 5 shows the resulting temperature evolutions for pure recoil heating ($\delta_{lc}=0$, resonant cavity), and for cavity heating ($\delta_{lc}=+\omega$) and cooling ($\delta_{lc}=-\omega$). The signature of cavity cooling is that the temperature after pumping on the cavity red sideband is smaller than the temperature after pumping on the cavity carrier, which is smaller than the temperature after pumping on the cavityblue sideband. Cavity cooling ($\delta_{lc}=-\omega$) counteracts recoil heating by free-space scattering, and results in a finite steady-state vibrational quantum number n_0=22. Fig. 5 also shows the prediction from the rate equation model of Refs. [33,34], where the fitted values agree with independent direct measurements.

Our results thus validate without free parameters the rate equation model [33,34], which predicts that it is possible to cavity cool atoms or ions to the motional ground state without decohering the internal state. This would require a large detuning of the laser compared to the atomic fine structure, a criterion which is easier to meet with light ions such as Be^+ [37].

3. Dynamic spin squeezing for an atomic clock

Sponsors
DARPA
National Science Foundation – Award ID number PHY 0653414

Squeezed spin states, collective states of an ensemble of spins whose total angular momentum has a component with less uncertainty than is possible for uncorrelated (unentangled) states, have attracted both theoretical and pragmatic interest since they were first proposed. [43-45]. From a fundamental physics perspective, they allow the study of many-body entanglement while retaining a simple theoretical description in terms of a single collective angular-momentum variable. In practical terms, they may offer a means of achieving measurement precision beyond the projection noise limit (standard quantum limit, SQL) [43,44], which was reached a decade ago by the best atomic clocks [46]. There have recently been several proof-of-principle demonstrations of spin squeezing using the Coulomb interaction between trapped ions [47], an optical quantum non-demolition (QND) [48,49] measurement [50,51], or collisions between atoms in a Bose-Einstein condensate [52]. Spin squeezing can be quantified by a metrological gain parameter that measures the improvement in signal-to-noise ratio over the SQL that takes into account the loss of signal due to decoherence during the squeezing process [43,44].

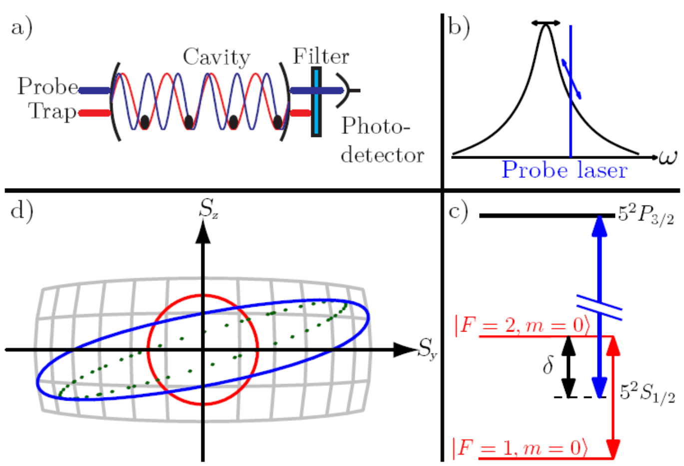

Figure 6. Method to implement cavity-induced dynamic spin squeezing. (a) The atoms are trapped in a standing-wave dipole trap inside the resonator. (b) The probe laser is detuned from (cavity) resonance by half a linewidth, so that atom-induced shifts of the cavity frequency cause changes in transmitted power. (c) The detuning of the cavity (and probe laser) is chosen halfway between the optical transition frequencies for the two clock states, so that the resonator frequency shift (and hence the change in transmitted power) is proportional toS_z. (d) The S_z-dependent Stark shift shears the circular uncertainty region of the initial coherent spin state (red circle) into an ellipse (dotted green line). Photon shot noise causes phase broadening that increases the ellipse area (solid blue line). The short axis of the ellipse is smaller than the width of the original coherent spin state (red). Curves are plotted for a modest shearing Q = 3.

We propose, analyze, and experimentally implement a simple dynamic squeezing method based on resonator-induced feedback. We show that a laser off-resonant from an atomic transition, and tuned to the slope of the cavity resonance, robustly and unconditionally squeezes the spin of an atomic ensemble inside the cavity. In analogy to one-axis twisting [45, 53], the light field inside the resonator induces a shearing of the Bloch sphere, which for an initial coherent spin state (CSS) results in reduced quantum noise along a specified direction (Fig. 6d). While photon shot noise in the incident light and photon scattering into free space are detrimental, substantial squeezing remains possible for large collective cooperativity (resonant optical depth). We have recently experimentally realized such a system, and observed unconditional spin squeezing in good agreement with the theoretical analysis [54].

Spin squeezing requires an interaction between the particles [45] that can be achieved by collective coupling of the ensemble to a light field [53,55], provided the sample's optical depth (opacity if probed on resonance) is sufficiently large. Such processes can be viewed as quantum coherent feedback [16], where the ensemble spin imprints its quantum fluctuations on the light field that then acts back on the spin state, creating quantum correlations (entanglement) in the spin variables.

The squeezing is produced by an ensemble-light interaction Hamiltonian of the form $c^{\dagger}cS_z$ that represents the differential light shift between two atomic levels due to the intracavity light with photon number $c^{\dagger}c$. The latter depends on the population difference $2S_z$ between the two atomic states through the tuning of the resonator mode by the atoms' index of refraction (see Fig. 6). In particular, if $c^{\dagger}c$ depends linearly on S_z, then the differential light shift between the two atomic states causes a precession of the spin vector about the z axis that is proportional to S_z. Then the initially circular uncertainty region of a CSS is sheared into an ellipse [45] as spin vectors of different S_z precess at different rates (Fig. 6d). The ellipse is narrower along one direction than the original CSS, corresponding to spin squeezing. The spin correlations between different atoms, i.e. the entanglement [45], arise from the fact that the quantum mechanical phase between the two states in any individual atom now depends on the population difference $2S_z$ of all atoms in the ensemble.

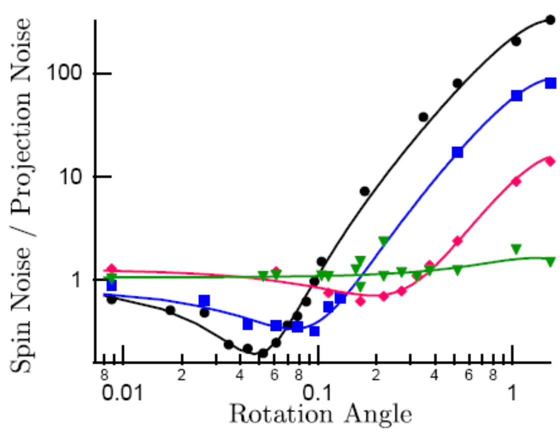

Figure 7.Observation of elliptical uncertainty region for different amounts of spin squeezing. The figure shows the measured readout variance $2\Delta S_z^2/S_0$ normalized to the projection noise $S_0/2$ of the initial coherent spin state (CSS). The triangles correspond to the circular uncertainty region of the CSS, the other data are for Increasing shearing Q=4.5 (red diamonds), Q=15 (blue squares) and Q=28 (black circles). The curves are sine waves fits (distorted by the double logarithmic scale).

We observe the shearing effect by rotating the state about the axis of its mean spin vector through a variable angle using a microwave pulse and recording the variance of a subsequent measurement of S_z over a series of 100 identical preparations. The readout of S_z is performed by measuring the cavity transmission on an avalanche photodiode, from which we can infer the shift of the cavity resonance frequency and hence S_z [57]. Typical data of variance as a function of rotation angle are displayed in Fig. 7. The variance is normalized to shot noise $N_0=2S_0$ (N_0 is the total atom number). The data are well described by sine wave fits, indicating that the uncertainty regions are indeed ellipses. As the state is rotated, the variance first dips below shot noise when the minor axis of the ellipse is rotated into alignment with *z,* and then increases beyond it as the major axis in turn is brought to vertical. The largest observed metrologically relevant spin squeezing [43,44], when the contrast loss in the spin squeezing process is taken into account, equals -6.0(3) dB, to our knowledge the largest squeezing observed in any spin system to date.

References

[1] R. Boyd, “Nonlinear Optics” (Academic Press, New York, 1992).

[2] D. Bouwmeester, A. K. Ekert, A. Z. (Editors), “The Physics of Quantum Information” (Springer, New York, 2000).

[3] R.F. Cregan, B.J. Mangan, J.C. Knight, T.A. Birks, P.S. Russell, P.J. Roberts, D.C. Allan, “Single-mode photonic band gap guidance of light in air,” Science **285**, 1537 (1999).

[4] B. Dayan, A. S. Parkins, T. Aok, E.P. Ostby, K.J. Vahala, H.J. Kimble, “A photon turnstile dynamically regulated by one atom,” Science **319**, 1062 (2008).

[5] K. M. Birnbaum, A. Boca, R. Miller, A. D. Boozer, T. E. Northup, H. J. Kimble, “Photon blockade in an optical cavity with one trapped atom,” Nature **436**, 87 (2005).

[6] T. Wilk, S. C. Webster, A. Kuhn, G. Rempe, “Single-Atom Single-Photon Quantum Interface,” Science **317**, 488 (2007).

[7] I. Fushman, D. Englund, A. Faraon, N. Stoltz, P. Petroff, and J. Vuckovic,” Controlled phase shifts with a single quantum dot,” Science **320**, 769 (2008).

[8] F. Benabid, G. Bouwmans, J. C. Knight, P. S. J. Russell, F. Couny, ” Ultrahigh Efficiency Laser Wavelength Conversion in a Gas-Filled Hollow Core Photonic Crystal Fiber by Pure Stimulated Rotational Raman Scattering in Molecular Hydrogen,” Phys. Rev. Lett. **93**, 123903 (2004).

[9] S. O. Konorov, A. B. Fedotov, A. M. Zheltikov, “Enhanced four-wave mixing in a hollow-core photonic-crystal fiber,” Opt. Lett. **28**, 1448 (2003).

[10] T. Takekoshi, R. J. Knize, “Optical Guiding of Atoms through a Hollow-Core Photonic Band-Gap Fiber,” Phys. Rev. Lett. **98**, 210404 (2007).

[11] S. Ghosh, A. R. Bhagwat, C. K. Renshaw, S. Goh, A. L. Gaeta, B. J. Kirby, “Low-Light-Level Optical Interactions with Rubidium Vapor in a Photonic Band-Gap Fiber,” Phys. Rev. Lett. **97**, 023603 (2006).

[12] R. Grimm, M. Weidemuller, Y. Ovchinnikov, “Optical dipole traps for neutral atoms,” Adv. At. Molec. Opt. Phys. **42**, 95 (2000).

[13] S. Harris, “Electromagnetically Induced Transparency,” Phys. Today **50**, 36 (1997).

[14] M. Fleischhauer, A. Imamoglu, J. Marangos, ” Electromagnetically induced transparency: Optics in coherent media,” Rev. Mod. Phys. **77**, 633 (2005).

[15] M. Fleischhauer, M. D. Lukin, “Dark-state polaritons in electromagnetically induced transparency,” Phys. Rev. Lett. **84**, 5094 (2000).

[16] L. Hau, S. Harris, Z. Dutton, C. Behroozi, “Light speed reduction to 17 metres per second in an ultracold atomic gas,” Nature **397**, 594 (1999).

[17] S. Harris, J. Field, A. Imamoglu, “Nonlinear optical processes using electromagnetically induced transparency,” Phys. Rev. Lett. **64**, 1107 (1990).

[18] H. Schmidt, A. Imamoglu, “Giant Kerr nonlinearities obtained by electromagnetically induced transparency,” Opt. Lett. **21**, 1936 (1996).

[19] M. Lukin, A. Imamoglu, “Controlling photons using electromagnetically induced transparency,” Nature **413**, 273 (2001).

[20] S. Harris, Y. Yamamoto, “Photon Switching by Quantum Interference,” Phys. Rev. Lett. **81**, 3611 (1998).

[21] D. Braje, V. Balic, G. Yin, S. Harris, “Low-light-level nonlinear optics with slow light,” Phys. Rev. **A 68**, 041801(R) (2003).

[22] D. James, P. Kwiat, "Atomic-Vapor-Based High Efficiency Optical Detectors with Photon Number Resolution," Phys. Rev. Lett. **89**, 183601 (2002).

[23] M. Bajcsy, A. S. Zibrov, M. D. Lukin, "Stationary pulses of light in an atomic medium," Nature **426**, 638 (2003).

[24] A. Andre, M. Bajcsy, A. S. Zibrov, M. D. Lukin, "Nonlinear Optics with Stationary Pulses of Light," Phys. Rev. Lett. **94**, 063902 (2005).

[25] D.E. Chang, V. Gritsev, G. Morigi, V. Vuletic, M.D. Lukin, and E. Demler, "Crystallization of strongly interacting photons in a nonlinear optical fiber," Nature Physics **4**, 884 (2008).

[26] F. Diedrich, J. C. Bergquist, W. M. Itano, and D. J. Wineland, "Laser Cooling to the Zero Point Energy of Motion," Phys. Rev. Lett. **62**, 403 (1989).

[27] S. E. Hamann, D. L. Haycock, G. Klose, P. H. Pax, I. H. Deutsch, and P. S. Jessen, "Resolved-Sideband Raman Cooling to the Ground State of an Optical Lattice," Phys. Rev. Lett. **80**, 4149 (1997).

[28] C. F. Roos, D. Leibfried, A. Mundt, F. Schmidt-Kaler, J. Eschner, and R. Blatt, "Experimental Demonstration of Ground State Laser Cooling with Electromagnetically Induced Transparency," Phys. Rev. Lett. **85**, 5547 (2000).

[29] A. Schliesser, R. Riviere, G. Anetsberger, O. Arcizet, and T. J. Kippenberg, "Resolved-sideband cooling of a micromechanical oscillator," Nature Phys. **4**, 415 (2008).

[30] D. J. Wineland, C. Monroe, W. M. Itano, D. Leibfried, B. E. King, and D. M. Meekhof, "Experimental issues in coherent quantum-state manipulation of trapped atomic ions," J. Res. Natl. Inst. Stand. Technol. **103**, 259 (1998).

[31] J. P. Home, M. J. McDonnell, D. J. Szwer, B. C. Keitch, D. M. Lucas, D. N. Stacey, and A. M. Steane (2008), "Memory coherence of a sympathetically cooled trapped-ion qubit," arXiv:0810.1036.

[32] P. Horak, G. Hechenblaikner, K. M. Gheri, H. Stecher, and H. Ritsch, "Cavity-Induced Atom Cooling in the Strong Coupling Regime," Phys. Rev. Lett. **79**, 4974 (1997).

[33] V. Vuletic and S. Chu, "Laser Cooling of Atoms, Ions, or Molecules by Coherent Scattering," Phys. Rev. Lett. **84**, 3787 (2000).

[34] V. Vuletic, H. W. Chan, and A. T. Black, "Three-dimensional cavity Doppler cooling and cavity sideband cooling by coherent scattering," Phys. Rev. **A 64**, 033405 (2001).

[35] T. Hänsch and A. L. Schawlow, "Cooling of gases by laser radiation," Opt. Commun. **13**, 68 (1975).

[36] R. A. Cline, J. D. Miller, M. R. Matthews, and D. J. Heinzen, "Spin relaxation of optically trapped atoms by light scattering," Opt. Lett. **19**, 207 (1994).

[37] R. Ozeri, C. Langer, J. D. Jost, B. DeMarco, A. Ben-Kish, B. R. Blakestad, J. Britton, J. Chiaverini, W. M. Itano, D. B. Hume, et al., "Hyperfine Coherence in the Presence of Spontaneous Photon Scattering," Phys. Rev. Lett. **95**, 030403 (2005).

[38] P. Maunz, T. Puppe, I. Schuster, N. Syassen, P. W. H. Pinkse, and G. Rempe, "Cavity cooling of a single atom," Nature **428**, 50 (2004).

[39] S. Nußmann, K. Murr, M. Hijlkema, B. Weber, A. Kuhn, and G. Rempe, "Vacuum-stimulated cooling of single atoms in three dimensions," Nature Phys. **1**, 122 (2005).

[40] K. M. Fortier, S. Y. Kim, M. J. Gibbons, P. Ahmadi, and M. S. Chapman, "Deterministic Loading of Individual Atoms to a High-Finesse Optical Cavity," Phys. Rev. Lett. **98**, 233601 (2007).

[41] H. W. Chan, A. T. Black, and V. Vuletic, Phys. Rev. Lett. **90**, "Observation of collective-emission-induced cooling of atoms inside an optical cavity," 063003 (2003).

[42] A. T. Black, H. W. Chan, and V. Vuletic, "Observation of Collective Friction Forces due to Self-Organization of Atoms: From Rayleigh to Bragg Scattering," Phys. Rev. Lett. **91**, 203001 (2003).

[43] D. J. Wineland, J. J. Bollinger, W. M. Itano, F. L. Moore, D. J. Heinzen, "Spin squeezing and reduced quantum noise in spectroscopy," Phys. Rev. **A 46**, R6797 (1992).

[44] D. J. Wineland, J. J. Bollinger, W. M. Itano, D. J. Heinzen, "Squeezed atomic states and projection noise in spectroscopy," Phys. Rev. **A 50**, R67 (1994).

[45] M. Kitagawa and M. Ueda, "Squeezed spin states," Phys. Rev. **A 47**, 5138 (1993).

[46] G. Santarelli, Ph. Laurent, P. Lemonde, A. Clairon, A. G. Mann, S. Chang, A. N. Luiten, and C. Salomon, "Quantum Projection Noise in an Atomic Fountain: A High Stability Cesium Frequency Standard," Phys. Rev. Lett. **82**, 4619 (1999).
[47] V. Meyer, M. A. Rowe, D. Kielpinski, C. A. Sackett, W. M. Itano, C. Monroe, and D. J. Wineland, "Experimental Demonstration of Entanglement-Enhanced Rotation Angle Estimation Using Trapped Ions," Phys. Rev. Lett. **86**, 5870-5873 (2001).
[48] A. Kuzmich, N. P. Bigelow, and L. Mandel, "Atomic quantum non-demolition measurements and squeezing," Europhys. Lett. **42**, 481-486 (1998).
[49] A. Kuzmich, L. Mandel, N. P. Bigelow, "Generation of Spin Squeezing via Continuous Quantum Nondemolition Measurement," Phys. Rev. Lett. **85**, 1594-1597 (2000).
[50] J. Appel, P. Windpassinger, D. Oblak, U. Hoff, N. Kjaergaard, and E. S. Polzik, "Quantum noise squeezing and entanglement on the atomic clock transition," Proceedings of the National Academy of Sciences **106**, 10960 (2009).
[51] M. H. Schleier-Smith, I. D. Leroux, and V. Vuletic, quant-ph/0810.2582 (2008).
[52] J. Esteve, C. Gross, A. Weller, S. Giovanazzi, and M. K. Oberthaler, "Squeezing and entanglement in a Bose-Einstein condensate," Nature **455**, 1216 (2008).
[53] M. Takeuchi, S. Ichihara, T. Takano, M. Kumakura, T. Yabuzaki, and Y. Takahashi, "Spin Squeezing via One-Axis Twisting with Coherent Light," Phys. Rev. Lett. **94**, 023003 (2005).
[54] I. D. Leroux, M. H. Schleier-Smith, and V. Vuletic, "Demonstration of Spin Squeezing by Cavity Feedback," to be submitted (2009).
[55] K. Hammerer, K. Mølmer, E. S. Polzik, and J. I. Cirac, "Light-matter quantum interface," Phys. Rev. **A 70**, 044304 (2004).
[56] H. M. Wiseman and G. J. Milburn, "Quantum theory of continuous feedback," Phys. Rev. **A 49**, 4110 (1994).
[57] M. H. Schleier-Smith, I. D. Leroux, and V. Vuletic, "Reduced-quantum-uncertainty states for an atomic clock," (2008), arxiv:quant-ph/0810.2582.

Publications

Journal Articles

Published:

"Crystallization of strongly interacting **photons i**n a nonlinear optical fiber," D.E. Chang, V. Gritsev, G. Morigi, V. Vuletic, M.D. Lukin, and E. Demler, Nature Physics **4**, 884 (2008).

"Efficient All-Optical Switching Using Slow Light within a Hollow Fiber," M.Bajcsy, S. Hofferberth, V. Balic, T. Peyronel, M. Hafezi, A.S. Zibrov, V. Vuletic, and M. D. Lukin, Phys. Rev. Lett. **102**, 203902 (2009).

"Observation of Cold Collisions between Trapped Ions and Trapped Atoms," A. Grier, M. Cetina, F. Orucevic, and V. Vuletic, Phys. Rev. Lett. **102**, 223201 (2009).

"Heralded Single-Magnon Quantum Receiver for Photon Polarization States," H. Tanji, S. Ghosh, J. Simon, B. Bloom, and V. Vuletic, Phys. Rev. Lett. **103**, 043601 (2009).

Submitted for publication:

"States of an Ensemble of Two-Level Atoms with Reduced Quantum Uncertainty," M. H. Schleier-Smith, I.D. Leroux, and V. Vuletic, submitted to Phys. Rev. Lett. (1/2009).

“Cavity Sideband Cooling of a Single Trapped Ion,” D. R. Leibrandt, J. Labaziewicz, V. Vuletic, and I. L. Chuang, accepted into Phys. Rev. Lett. (7/2009).

“Trapping and manipulation of isolated atoms using nanoscale plasmonic structures,“ D.E. Chang, J.D. Thompson, M.D. Lukin, H. Park, V. Vuletic, A.S. Zibrov, and P. Zoller, submitted to Phys. Rev. Lett. (5/2009).

“Fast Entanglement Distribution with Atomic Ensembles and Fluorescent Detection,” J.B. Brask, L. Jiang, A.V. Gorshkov, V. Vuletic, A.S. Sorensen, M. D. Lukin, submitted to Phys. Rev. Lett.

Meeting Papers

“Heralded atomic-ensemble quantum memory for photon polarization states,” J. Simon, H. Tanji, S. Ghosh, B. Bloom, and V. Vuletic, Phys. Scr. **T134**, 000000 (2009).

“Few-photon switching with slow light in hollow fiber,” M. Bajcsy, S. Hofferberth, V. Balic, T. Peyronel, M. Hafezi, A. S. Zibrov, V. Vuletic, M.D. Lukin, published in: Proc. of SPIE, Vol. **7226** (Advances in Slow and Fast Light II), 722609 (2009).

“Producing Squeezed Input States for an Atomic Clock Using an Optical Cavity,” I.D. Leroux, M.H. Schleier-Smith, and V. Vuletic, in: Proceedings of the Joint Meeting of the European Frequency and Time Forum and the IEEE International Frequency Control Symposium (EFTF/IFCS), Besancon, France (2000).

“Switching of light with light using cold atoms inside a hollow optical fiber,” M. Bajcsy, S. Hofferberth, T. Peyronel, V. Balic, M. Hafezi, A. S. Zibrov, M. D. Lukin, and V. Vuletic, to be published in Proceedings of the 19th International Conference on Laser Spectroscopy (ICOLS 2009, Hokkaido, Japan), edited by H. Katori.

“Preparation of Reduced-Quantum-Uncertainty Input States for an Atomic Clock,” M. H. Schleier-Smith, I. D. Leroux, and V. Vuletic, published in Proceedings of SPIE (2009).